Journal of Medicinal Chemistry

pubs.acs.org/jmc

Perspective

Does the Number of Bifunctional Chelators Conjugated to a mAb Affect the Biological Activity of Its Radio-Labeled Counterpart? Discussion Using the Example of mAb against CD-20 Labeled with ^{90}Y or ^{177}Lu

Urszula Karczmarczyk,* Agnieszka Sawicka,* Piotr Garnuszek, Michał Maurin, and Wioletta Wojdowska

Cite This: *J. Med. Chem.* 2022, 65, 6419–6430

Read Online

ACCESS | Metrics & More | Article Recommendations

ABSTRACT: There has been considerable interest in developing a monoclonal antibody (mAb) against-CD-20 (for example, Rituximab) modified by bifunctional chelating agents (BCA) for non-Hodgkin's lymphoma radioimmunotherapy. Therefore, many researchers have modified this monoclonal antibody by attaching different BCA moieties and evaluated their biological activities in terms of in vitro study and in vivo study in healthy and tumor xenografted rodents. This mini-perspective reviews the in vitro studies, the immunoreactivity and physiological distribution studies: organ-to-blood and the tumor-to-organ ratio of conjugates with different numbers of chelators per mAb. We set up a null hypothesis that states there is no statistical significance between the biological activity of monoclonal antibody (Rituximab) and the number of conjugated bifunctional chelators. Overall, we have concluded that there is no strong evidence for this hypothesis. However, the literature data should be questioned due to the potential lack of uniform study methodology.

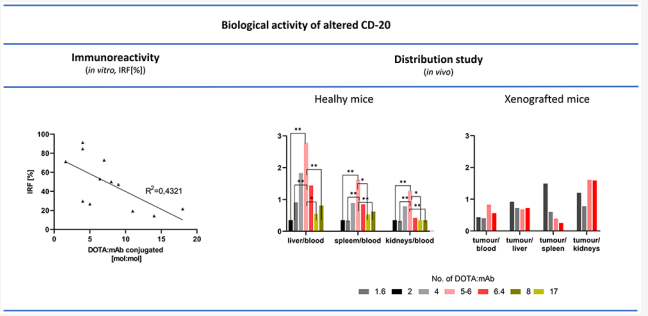

INTRODUCTION

Monoclonal antibodies are the type of immunotherapeutics that work by triggering the immune system and helping it attack cancer.[1−3] They act through one of the following mechanisms: the blockade of oncogenic pathways with subsequent effects on cell growth and apoptosis,[4,5] blocking angiogenesis,[6,7] modulation of the immune response,[8] the regulation of osteoclast function,[9] delivery of the small molecule payloads to specific cell types,[10] or recruitment of immune cells to cancer cells, and more.

Since the approval of the first mAb against CD20 (Rituximab) by the United States Food and Drug Administration (FDA) for clinical use in the therapy of cancer in 1997,[11] hundreds of mAbs, including murine, chimeric, humanized, and human, have been available for clinical use in everyday practice as a monotherapy, in combination with standard chemotherapy or for theranostic application as radiolabeled monoclonal antibodies.[12,13]

The B-lymphocyte antigen CD20 is a transmembrane protein, expressed on the surface of all B-cells beginning at the pro-B phase (CD45R+, CD117+) and progressively increasing in concentration until maturity.[14] CD20 is the target of monoclonal antibodies like Rituximab which are all active agents in treating all B cell lymphomas, leukemias, and B cell-mediated autoimmune diseases. Due to the promising results obtained in patients with non-Hodgkin's lymphoma (NHL), radiolabeled monoclonal antibodies have been actively investigated for radioimmunotherapy (RIT). The studies concerning NHL revealed high intrinsic radiosensitivity, excellent access of the radiolabeled mAbs to the tumor cells and the inherent antitumor activity.[15]

These studies have resulted in the first registered radiolabeled mAbs directed for the surface antigen CD-20-^{90}Y-labeled anti-CD20 mAb Zevalin (CTI BioPharma Corp., Seattle, WA, U.S.A.) and ^{131}I-labeled anti-CD20 mAb Bexxar (Corixa, Seattle, WA, U.S.A.).[16,17] However, despite the success of the mentioned drugs, several questions about the optimization of the radiopharmaceutical preparation and radiolabeled monoclonal antibodies in NHL remain open. In addition, more profound knowledge of the mechanisms underlying resistance to mAb is also necessary.

Received: November 30, 2021
Published: April 20, 2022

https://doi.org/10.1021/acs.jmedchem.1c02044
J. Med. Chem. 2022, 65, 6419−6430

The preparation of a new radiotracer begins with an optimization process to select the suitable bifunctional chelating agent (BCA), which, in the case of Rituximab, commonly involves polyaminocarboxylic acid (DTPA) or 1,4,7,10-tetraazacyclododecane-*N*,*N*′,*N*′,*N*′-1,4,7,10-tetraacetic acid (p-NCS-Bz-DOTA) or *N*-hydroxysulfosuccinimidy (DOTA-SCN), for complexation of trivalent (^{90}Y, ^{177}Lu) or divalent (^{67}Cu) metal ions.[18] Furthermore, to improve the radiolabeling efficiency, it is preferable to conjugate a high amount of chelator per mAb, which delivers the required therapeutic dose of radiometal with a decreased amount of immunoconjugate.

However, the high conjugation ratio (chelator/conjugation of more chelator to mAb can alter the physical, biological, and immunological properties of the mAb, consequently affecting its tumor-targeting pharmacokinetics. For example, the changes in physical properties described by Pham et al. show that the conjugation of DTPA could increase net negative charges in the mAb, thereby decreasing the isoelectric point (pI) of the mAb.[19] The second limitation caused by the increased ratio of the chelator to mAb is the probability of decreasing the binding affinity of the mAb to its antigen.[20] Finally, a high number of chelators attached to mAb may change the in vivo clearance pharmacokinetics due to the uptake of the conjugate by the reticuloendothelial system in the liver and spleen.[21] It should be remembered that not only do physicochemical properties influence the in vivo nature of immunoconjugate, but it can also be affected by biological factors such as blood flow, tumor size, tumor microenvironment (TEM), permeability, or concentration gradient between the blood and tumor.

This mini-perspective sets up a null hypothesis stating there is no statistical significance between the biological activity of monoclonal antibody (CD-20) and the number of conjugated bifunctional chelators.

CHELATORS

Bifunctional chelators contain two moieties—multidentate for metal chelatation and the one capable of conjugating with biologically active targeting molecules such as peptides, nucleotides, antibodies, or nanoparticles. In the most common bioconjugation techniques, the functional groups such as carboxylic acids, activated esters for amide coupling, isothiocyanates for thiourea couplings, or maleimides for thiol couplings are employed.

Designing the core structure and conjugative unit of BCAs depends on their application area. Different chelating agents vary from simple acyclic to complex macrocyclic units. Macrocycles tend to be more kinetically inert than acyclic chelators, although their thermodynamic stabilities are proven to be similar.[22,23] The further advantage of macrocyclic over acyclic chelators is that they require much less physical manipulation to arrange donor atoms to coordinate with a metal ion. However, acyclic chelators show better complexation kinetics and radiolabeling efficiency in low temperatures. The radiometal coordination can be completed in 15 min at room temperature, whereas macrocyclic compounds often need an elevated temperature up to 95 °C and prolonged reaction time (15 min). These properties are crucial when handling heat-sensitive molecules such as antibodies or labeling with short half-life isotopes such as ^{68}Ga, $^{212/213}$Bi, ^{44}Sc, or ^{64}Cu.

DTPA is one of the most extensive used acyclic chelators in radiochemistry. However, as a first-generation radiometal chelator, it shows lower stability in vivo with many radiometal ions than macrocyclics like DOTA and NOTA. The novel derivatives have been designed to overcome these shortcomings, such as 1B4M-DTPA and CHX-A″-DTPA.[24,25] A single methyl group on one of 1B4M-DTPA's ethylene backbones and the cyclohexyl backbone of the CHX-A″-DTPA enhance kinetic inertness but retarding radiolabeling kinetics compared to those of DTPA.[26,27]

The most commonly used chelator to this day is probably DOTA. Although this macrocyclic chelator requires elevated temperature for radiolabeling, its exceptional in vivo stability and the commercial availability of many different bifunctional DOTA derivatives and vector conjugates make it the "gold standard" for many isotopes, including ^{111}In, $^{86/90}$Y, ^{225}Ac, $^{44/47}$Sc, and ^{177}Lu. Both Y^{3+} and Lu^{3+} preferentially form 8−9 coordinate complexes in square antiprismatic or capped square antiprismatic geometries and are hard metal ions with a preference for hard ligand donors such as carboxylate-oxygens and amine-nitrogens.

The covalent bond between chelator and mAb is generally robust, and the BCAs are designed to coordinate the radionuclide stably.[28−30]

MEASUREMENT OF THE NUMBER OF THE CHELATORS PER MONOCLONAL ANTIBODY

There is no doubt that the biological activity of mAb may be decreased by inappropriate attachment of chelators or by radiolabeling conditions. Furthermore, many researchers claim that the level of mAb's altering, which translates to immunoreactivity, increases with increasing substitution.[20,31] Moreover, the increased metal ion chelation, the net charge, and the hydrodynamic radius result from the increasing DOTA/antibody conjugation ratio. Therefore, to assess scientifically comparable and valuable results, it is very important to determine the number of chelator groups attached to a monoclonal antibody and assess the conjugate's biological activity.

The most popular procedure for determining the number of DOTA molecules conjugated to the antibody is the colorimetric method measuring the absorbance of a solution containing complexes of metal ions (such as Cu^{2+}, Pb^{2+}, Y^{3+}, or Tb^{3+}) and Arsenazo(III). It measures the number of mAb-bound metal chelator molecules available for metal binding.[30,32−41] Those methods bring some benefits like simplicity and relatively fast determination. However, the main limitation is the low sensitivity in the micromolar range, so the accuracy of the DOTA/mAb ratio is very low.

Alternatively, the number of attached DOTA groups may be determined by MALDI-TOF MS calculations,[42] size-exclusion HPLC (SE HPLC),[42] or radioassay (HPLC) using cold $^{89}YCl_3$ $6H_2O$.[35,43]

The basis of MALDI-TOF is mass spectrometry, which comprises three main components: an ion source to ionize and transfer sample molecules ions into a gas phase, a mass analyzer device that separates molecules depending on their mass, and a detector to monitor all separated ions. The advantages of this method are rapid turnaround time (<10 min) and a wide range of analyzed masses. However, the best use is to determine MW > 1 kDa, which could be interpreted as a disadvantage.

It is worth noticing that the calculated number of chelators per Rituximab is only statistically averaged. This is because the chelators are not shared equally in the mAb molecule under the assumption that Poisson distribution apply. Considering that the results describing the number of chelators attached per

https://doi.org/10.1021/acs.jmedchem.1c02044
J. Med. Chem. 2022, 65, 6419−6430

Rituximab are based on different methods, it is not easy to compare the literature data and draw reliable conclusions. For that reason, we have calculated the correlation only for results obtained using the spectroscopic method, but we also put on the chart the results obtained using nonspectroscopic methods, Figure 1.

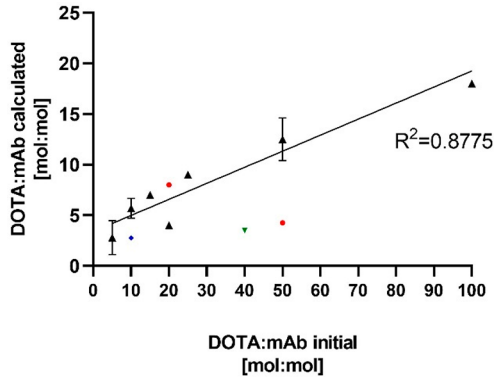

Figure 1. Quantity of calculated DOTA chelators per mAb-based on the initial amount of DOTA and different analytical methods, based on data listed in Table 1. Linear correlation (R^2 = 0.8775) refers to data calculated using the spectrophotometric method (▲). The correlation does not consider the marked as (▼, spectrophotometric method), (♦, HPLC method), and (●, MALDI SM method).

As shown in Figure 1, the higher amount of initial DOTA chelators per mAb results in a higher number of DOTA bound to a monoclonal antibody, with the linear regression equal to R^2 = 0.8775. This observation is based on the independent laboratory results obtained under nonstandardized analytical protocols. It is worth emphasizing that the outcome based on different methods will not be similar.

The researchers increased the number of metal-binding sites per antibody to decrease the amount of immunoconjugate, in mg, required to deliver a therapeutic dose of radiometal. Furthermore, the low amount of injected tracer (picomoles to nanomoles, sum of radioactive, and stable molecules) enables one to omit the pharmacologic effects. Nevertheless, the pharmacokinetics of the antibody can be modified by the higher conjugation of the hydrophilic DOTA chelator.

COMPARISON OF MODIFIED RITUXIMAB IMMUNOREACTIVITY

Immunoreactivity is defined as reacting to particular antigens or haptens.[44] The conjugation of chelating agents to a mAb as well as labeling procedure or radiolysis during mAb storage may adversely alter the antibody and affect the immunoreactivity. In this way, unfavorable in vivo behavior of radioimmunopharmaceuticals, such as reduced tumor uptake, increased nonspecific localization and radiation exposure of nontarget tissues, can be identified. Therefore, the determination of immunoreactive fraction (IRF) is essential to ensure the efficacy of radiolabeled antibodies. The method of determining the IRF should be simple, reproducible, and robust.

The conventional method to pinpoint an immunoreactive fraction is based on the radioimmunoassay technique in which the fraction of radiolabeled mAb bound to antigen under conditions of "antigen excess" is determined. The relative binding (bound antibody over total antibody [B]/[T]) is a function of increasing antigen (or tumor cells) concentration [F]. Under conditions of extreme antigen excess, the relative binding at saturation approximates the IRF. Lindmo et al. developed the binding assay in which the immunoreactive fraction is assessed by saturating the radioimmunoconjugate with an increasing excess of antigen, followed by linear extrapolation to infinitive antigen excess.[45] It is thus assumed that the Lindmo method allows the estimation of the true value of the IRF, unlike an apparent IRF determined under the condition of limited antigen excess. Immunoreactive fraction is calculated using a double reciprocal of the total antibody number over bound antibody against the inverse cell concentration (1/[cells]). The inverse of the Y-intercept equals the immunoreactive fraction. Although the Lindmo assay is the most commonly applied, it has revealed considerable criticism.[46−48] The Lindmo extrapolation sometimes produces results that appear unreliable and overestimated, which indicates the method's sensitivity to experimental conditions. The analysis is conducted under significant antigen excess so that the

Table 1. Results of Immunoreactivity Obtained by Different Research Groups

chelator	molar excess of chelator	average number of attached chelator	method of assessing the chelator number	IRF (%)	ref.
DOTA-NHS	50:1	14	spectrophotometric	14.3 ± 2.9	55
	100:1	18		20.4 ± 2.1	
p-SCN-Bz-DOTA	10:1	5		26.8 ± 5.4	
p-SCN-Bz-DOTA	10:1	1−1.5	SE HPLC		54
	50:1	4.25 ± 1.0		(70% declared) 111.6	
p-SCN-Bz-DOTA	5:1	1	radioassay-HPLC		42
	10:1	4	MALDI-MS	84.7	
	20:1	8		50.0	
p-SCN-Bz-DOTA	5:1	4	spectrophotometric	91.4	36
	15:1	7		72.8	
	25:1	9		47.3	
p-SCN-Bz-DOTA	5:1	1.6 ± 0.5	spectrophotometric	71.2	30
	10:1	6.4 ± 1.7		53.1	
	50:1	11.0 ± 2.6		19.4	
DOTA-NHS	~40:1	3.5	spectrophotometric	(85% declared) 55	39
p-SCN-Bz-DOTA	10:1		spectrophotometric		38
	20:1	4		(70% declared) 29.8	

https://doi.org/10.1021/acs.jmedchem.1c02044
J. Med. Chem. 2022, 65, 6419−6430

concentration of total antigen approximates the concentration of the free antigen. However, experimental conditions such as a small number of antigen molecules per cell and/or low affinity of antibodies invalidate this approximation and cause systematic errors in the measurement of IRF. The other factor that significantly impacts the estimation of IRF is the specific activity or the amount of antibody mass used for the cell-binding assay. The linear relationship of [T]/[B] as a function of the inverse concentration of free antigen (1/[F]) is only true when the binding reaction has been allowed to reach equilibrium. Therefore, optimization is necessary using a conventional plat for each tested preparation. The effect of some variables, including mAb mass, specific activity, antigen or cell concentration, and incubation time on the determination of IRF by the Lindmo method, was previously evaluated by Konishi et al.[48] They also propose the alternative method where a fixed antigen amount (under the condition of limited antigen excess) and varying concentrations of radiolabeled antibodies are implemented. Thus, the relative binding ([B]/[T]) is plotted as a function of total mAb concentration, and a curve in which the % bound ([B]/[T]) is higher at low mAb concentration and decreases as the mAb concentration increases.

In the present work, we analyze the influence of the chelator molecule number (chelator: antibody ratio, c/a) on the immunoreactivity of Rituximab radiolabeled with ^{177}Lu or ^{90}Y studied by different researches groups. The summary of the reviewed studies is shown in Table 1. Generally, it has been observed the c/a at which the immunoreactivity is significantly reduced varies depending on the type of chelating agent or linker and with conjugation reaction.[49−52]

The mini-perspective compares the results from our in vitro studies and literature data. In our research, Rituximab (MabThera) was conjugated with two different macrocyclic chelators p-NCS-Bz-DOTA or DOTA-NHS and then labeled with lutetium-177. Immunoreactivity of [^{177}Lu]Lu-p-SCN-Bz-DOTA-Rituximab and [^{177}Lu]Lu-DOTA-NHS-Rituximab was determined by the method of Lindmo using Raji cell line. Rituximab was conjugated with ten times molar excess of p-NCS-Bz-DOTA and 50 and 100 times molar excess of DOTA-NHS.[54] The immunoreactivity was 26.8 ± 5.4% for [^{177}Lu]Lu-p-SCN-Bz-DOTA-Rituximab (5 molecules attached) and 14.3 ± 2.9% and 20.4 ± 2.1% for [^{177}Lu]Lu-DOTA-NHS-Rituximab for 14 and 18 DOTA-NHS molecules, respectively.[53]

In the study of Thakral et al., the immunoconjugate of biosimilar Rituximab (Reditux) and p-NCS-Bz-DOTA was prepared and radiolabeled with lutetium-177.[54] Antibody was incubated with p-NCS-Bz-DOTA in 1:10 and 1:50 molar ratios for 30 min at 37 °C. The conjugation mixture was purified using a PD10 column (0.25 M ammonium acetate, pH 5−5.5) to remove unconjugated p-NCS-Bz-DOTA. The number of p-NCS-Bz-DOTA molecules attached to a single antibody molecule was determined using SE HPLC method. When the antibody to chelator ratio was 1:10, an average of 1−1.5 molecules of p-NCS-Bz-DOTA was conjugated to one Rituximab molecule. As the authors claim, this amount was insufficient for prompt labeling with Lu-177. The mAb: chelator ratio 1:50 resulted in the stoichiometry of 4.25 ± 1.04 DOTA-SCN molecules attached to each antibody molecule. The immunoreactivity of ^{177}Lu-labeled DOTA-Rituximab was determined by the Lindmo method with RAMOS cell in five concentrations (0.5×10^7 to 3.13×10^5). The conjugation process was carried out overnight at 4 °C with 5−7.5 ng of [^{177}Lu]Lu-DOTA-Rituximab. The binding of the immunoconjugate increased in a parabolic pattern. The authors claimed that the immunoreactivity was approximately 70% at the highest cell concentration. The Lindmo plot was defined by equation $y = 0.3643x + 0.8957$, $R^2 = 0.7984$. Because the immunoreactivity fraction is given by the reciprocal of the intercept on the ordinate, it should be 111% for this study.

Forrer et al. evaluated the immunoconjugate DOTA-Rituximab as a kit formulation that could be labeled in a short time (<20 min) with both ^{177}Lu or ^{90}Y.[42] The Rituximab (MabThera) was conjugated with p-SCN-Bz-DOTA at 37 °C and pH 9.5 for 1 h in molar ratios of 1:5, 1:10 and 1:20. The solution was washed several times with 0.25 M ammonium acetate, pH 7. The immunoconjugate solution was prepared in kit form by lyophilization. The DOTA/mAb ratio was determined using $^{57}Co/CoCl_2$ (1:5 and 1:10 ratio) and $^{177}Lu/^{nat}LuCl_3$ (1:10 ratio) solutions. Additionally, matrix-assisted laser desorption ionization mass spectroscopy (MS MALDI) was performed to determine the number of chelators per antibody molecule. An average of four DOTA molecules per Rituximab molecule [$(DOTA)_4$-Rituximab] was found in the case of conjugation in a 1:10 molar ratio. The 20-fold excess of p-NCS-Bz-DOTA during the coupling reaction resulted in an average number of eight DOTA molecules per antibody [$(DOTA)_8$-Rituximab]. The unconjugated Rituximab and the reconstituted kit of DOTA-Rituximab were desalted by centrifugation at 4 °C using Ultra-15 filters and washed numerous times with water. The immunoreactivity of the DOTA-Rituximab immunoconjugate before labeling was analyzed by flow cytometry. The binding of kits containing four or eight DOTA molecules per antibody molecule to the CD20-transfected cell line L-VB1 was compared with the unconjugated Rituximab antibody. The authors observed no significant influence of $(DOTA)_4$-Rituximab on the immunoreactivity compared to the unconjugated Rituximab. With the immunoconjugate $(DOTA)_8$-Rituximab, the binding was drastically (50%). To determine the immunoreactive fraction of the radiolabeled Rituximab, an immunoreactivity assay described by Lindmo et al. was adopted. For the [^{177}Lu]Lu-$(DOTA)_4$-Rituximab concentration of 1 ng/mL, the L-VB1 cells concentrations were 3.2, 1.6, 0.8, 0.4, 0.2, and 0.1×10^5 cells/ml. The plates were incubated at 37 °C for 2 h. The immunoreactive fraction, calculated from a double inverse plot and described by the equation $y = 0.066x + 1.181$, was 84.7%. This observation indicates that most of the radiolabeled antibody is immunoreactive, possessing a high binding affinity for the CD20 antigen of lymphoma cells.

In the other study described by Gholipour et al.,[36] Rituximab was conjugated with p-NCS-Bz-DOTA in carbonate buffer (pH 9.5) in molar ratios of 5, 15, and 25 at room temperature for 24 h. Then, the unreacted p-NCS-Bz-DOTA was removed by ultrafiltration and washing with ammonium acetate buffer (0.25 M, pH 5.5). Finally, the formulated immunoconjugate solutions were freeze-dried. The number of DOTA molecules attached to the antibody, determined based on a transchelation between DOTA and arsenazo yttrium(III) complex from a standard curve for absorbance of Arsenaso yttrium(III) complex, was 4, 7, and 9 for Rituximab: DOTA ratios 1:5, 1:15 and 1:25, respectively. The conjugate was labeled with ^{90}Y and ^{111}In. The Lindmo method on the Raji cell line determined the immunoreactivity of radioimmunoconjugates, using five sequential dilutions of 10^6-10^7cells. The average immunoreactivity for radioimmunoconjugates decreased by an increase in DOTA:Rituximab molar ratios and were 91.4%, 72.8%, and

https://doi.org/10.1021/acs.jmedchem.1c02044
J. Med. Chem. 2022, 65, 6419−6430

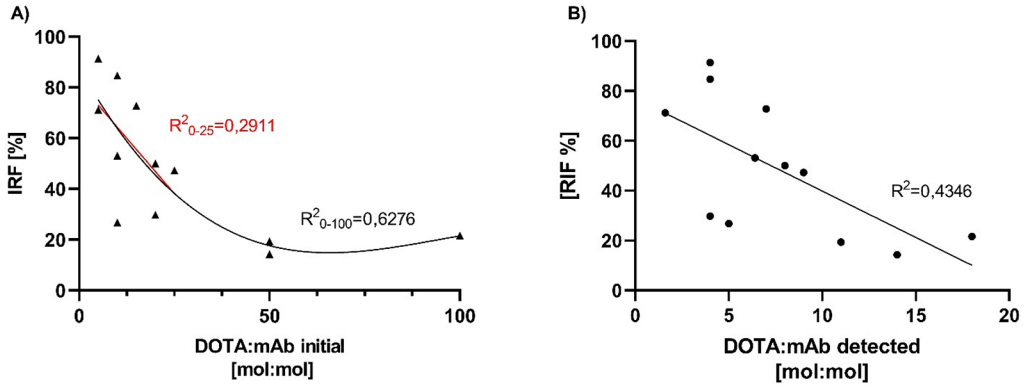

Figure 2. Scatterplot of IRF and number of initial (A) and detected (B) DOTA molecules to Rituximab, based on data listed in Table 1. There are two correlation lines in part (A): first is for DOTA: mAb ratio range from 0 to 25 (red line R^2_{0-25}), and second is for DOTA:mAb ratio range from 0 to 100 (black line R^2_{0-100}).

47.3%, for approximate conjugation of 4, 7, and 9 DOTA molecules, respectively.

Guleria et al.,[30] the next research group, evaluated the effect of the number of p-NCS-Bz-DOTA present per antibody molecule on the pharmacokinetics and immunoreactivity of the ^{177}Lu-labeled Rituximab (BioSim, Reditux). Coupling was carried out in three different antibody ratios to a chelator, that is, 1:5, 1:10, and 1:50. For the preparation of conjugates corresponding to 1:10 and 1:50 mAb to BCA molar ratios, the reaction mixtures were incubated at 37 °C, in 0.2 M sodium carbonate-bicarbonate buffer pH 9.5 for 17 h. For the antibody to chelator ratio 1:5, the reaction was performed 3 h at the same conditions. Rituximab-p-NCS-Bz-DOTA conjugates were purified using PD-10 Sephadex G-25 M columns eluting with a 0.1 M ammonium acetate buffer (pH 5.5). The average number of p-NCS-Bz-DOTA molecules attached per antibody moiety was determined by a spectrophotometric assay. The number of attached DOTA molecules was 1.62 ± 0.5, 6.42 ± 1.72 and 11.01 ± 2.64 in the conjugates obtained at 1:5, 1:10, and 1:50 molar ratios of Rituximab and p-NCS-Bz-DOTA, respectively. Determination of immunoreactive fractions was conducted according to the Lindmo method. For this purpose, Raji cells (5×10^6 to 20×10^6) were incubated with p-NCS-Bz-DOTA at 4 °C for about 2 h. The following %IRF values could be calculated from the graphs: 71.17, 53.05, and 19.37 for 1.62 ± 0.50, 6.42 ± 1.72, and 11.01 ± 2.64 average number p-NCS-Bz-DOTA per Rituximab, respectively.

Daha et al.[39] examined the immunoreactivity of ^{177}Lu labeled Rituximab on Raji cells using ^{177}Lu-Rituximab conjugated to 3.5 DOTA-NHS molecules. The conjugation process was carried out in borate buffer at pH 8−8.5 for 24 h at 2−8 °C in the chelator's 50:1 molar excess. The complex was purified by 24 h dialysis against 0.25 M ammonium acetate buffer, and the number of DOTA molecules was determined by a spectroscopic assay using Arsenazo reagent. The author states the IRF as ca. 85.5%, although according to the Lindmo plot ($y = 1.35x + 1.81$, $R^2 = 0.989$), the immunoreactive fraction was 55% (one divided by 1.81).

In the other study described by Doha et al.,[38] the authors determined the immunoreactivity of Rituximab (Zytux, Aryogen Biopharma) conjugated to p-NCS-Bz-DOTA and labeled with ^{90}Y. The conjugation process was carried out in carbonate buffer (pH 8.6) in the molar ratio mAb/DOTA 1:20 or 1:10 at room temperature overnight or at 37 °C for 1−2 h. Excess of DOTA was removed using a Centricone filter. The number of DOTA molecules conjugated per Rituximab molecule was determined using the spectrophotometric method based on the Arsenazo-(III)-Pb(II) complex. The conjugation of 20-fold DOTA to Rituximab resulted in approximately four DOTA per antibody. To determine the affinity (K_d) of radiolabeled antibody to CD20 on Raji cells, the maximum number of antibody molecules bound per cell saturation binding studies were conducted. The equilibrium dissociation constant K_d was calculated as 2.8 ± 0.46 nM and the receptor density B_{max} as 0.6 ± 0.03 pmol per 10^6 cells, which indicates that approximately 3.6×10^5 molecules of [^{90}Y]Y-DOTA-Rituximab can be bound per cell at saturation. The IRF of the complex was determined using the Lindmo method. For this purpose, a series of increasing concentrations of cells were incubated with a 200-fold dilution of the saturation concentration of [^{90}Y]Y-DOTA-Rituximab for 2 h at 4 °C. The author assumes the IRF of approximately 70%, although according to the equation $y = 13.305x + 3.3581$, it is nearly 30%.

Analyzing the literature data, two ways of determining the impact of chelator number on immunoreactivity could be noted. First, immunoreactivity as a function of the initial number of chelators taken for conjugation, Figure 2A, or second, immunoreactivity as a function of the determined number of chelators attached to the mAb, Figure 2B.

In both cases, we can observe that the increased DOTA:mAb ratio decrease the IRF. In Figure 2A, the scatter plot shows that the increase of the initial amount of BCA above 50 does not influence immunoreactivity, which remains at level c.a. 20%. In Figure 2B, the scatter plot shows the statistically significant (p = 0.0074) correlation between immunoreactivity and the determined number of chelators (in the range from 0 to 25) attached to the mAb. R square (R^2; Pearson's correlation) equals 0.4321, revealing a low negative correlation between IRF and the number of attached DOTA to Rituximab. We extracted from scatter plot 2A (X-axis from 0 to 100), part for X-axis from 0 to 25, and calculated the correlation for this range of DOTA: mAb initial molar ratio. In that case, we can claim a very low, statistically insignificant (p = 0.1338), negative correlation between IRF and the DOTA: initial mAb ratio in the range equal 0.2911 (Figure 2A, red line).

To sum up, a chemical modification of mAb and the type of the cell line applied for the study may affect these immunoreactivity results. For statistical analysis, linear regression and Pearson's correlation were performed using GraphPad Prism version 8.00 for Windows.

https://doi.org/10.1021/acs.jmedchem.1c02044
J. Med. Chem. 2022, 65, 6419−6430

Table 2. Animals Model for Radiolabelled Rituximab Study

animal	tumor	chelator	injected dose	ref.
Rats male		p-NCS-Bz-DOTA		36
Rats		DOTA-NHS	<6 μg, 3.7 MBq	68
Rats		DTPA anhydride		23
Rats		DTPA	0.74 MBq	71
Rats Nude female	MC116 B	Zevalin (DTPA)		70
Swiss mice		p-NCS-Bz-NOTA	0.37−0.44 MBq ^{68}Ga-NOTA-F(ab′)-Rituximab ^{68}Ga-NOTA-F(ab′)2-Rituximab	37
Swiss mice		p-NCS-Bz-DOTA	100 μL, 3.7 MBq	30
BALB/c mice		p-NCS-Bz-DOTA	50 μg, 3.7 MBq	38
BALB/c		p-NCS-Bz-DOTA	10 μg, 2 MBq	75
Normal mice		DOTA-NHS	50 μg, 37 MBq	39
Swiss mice		p-NCS-Bz-DOTA		43
CD-1 mice		sulfo-NHS		72
BALB/c Nude male		p-NCS-Bz-DOTA	1−0.1−0.01 μg kg^{-1}	73
SCID mice	Raji	CHX-A′′-DTPA	0.37−0.55 MBq	40
BALB/c Nude female	Daudi	p-NCS-Bz-DOTA	1−0.1−0.01 μg kg^{-1}	73
BALB/c Nude	Raji	p-NCS-Bz-DOTA DOTA-NHS	10 μg, 6 MBq	41
BALB/c Nude	Raji Jurkat	p-NCS-Bz-DOTA DOTA-NHS	10 μg, 6 MBq	29

COMPARISON OF IN VIVO STUDIES

A variety of animal models for human diseases play essential roles in biomedical research, including lymphoma and the development of new drugs for these diseases.[56] The most common murine lymphoma model is transplantable and genetically engineered mouse models. Transplantable models, either syngeneic (implantation of murine cell lines),[57,58] or xenograft (transplantation of human cells),[59] require a systematic approach (that is, cells can be administered via subcutaneous, orthotopic, intraperitoneal, or intravascular route) and bring both benefits and drawbacks.[60−62] Xenograft mouse models are applied in immunocompromised mice ranging from athymic nude to variation on severe combined immunodeficiency (SCID) mice. Nude mice are generated on BALB/c background utilizing a mutation in Fox,[1] resulting in the lack of thymic development (mice still carry B cells). In contrast, SCID mice are typically ΔPrkdc and Rag[1] null derived on a C57BL/6, C3H, or nonobese diabetic/LtSzJ backgrounds (mice result in the lack of functioning B and T cells with minimal to no NK activity).[63] However, using the xenograft mouse model based on cell lines does not guarantee the primary tumor characteristic.[64] The humanized mouse model or genetically engineered one is an alternative to overcome this drawback,[65,66] for example, mice bearing the cellular myc oncogene coupled to the immunoglobulin μ or κ[67] and mice with Vav gene regulatory sequences to drive Bcl-2 expression in the development of follicular lymphoma.[68]

A few literature reports cover the use of rats in research on radiolabeled Rituximab,[36,69−72] but the overwhelming majority of the reports relate to the murine model, Table 2. The latter model encompasses both healthy[30,37−39,43,73,74] and immunodeficient mouse strain, that is, NOD/SCID and Nude.[29,40,41,75] Transplantable xenograft models were subcutaneously grafted with RAJI, DAUDI, or RAMOS cells from existing cell lines, not from the primary tumor origin (patient-derived). The advantage of this approach was undoubtedly rapid result, relative simplicity, high yield, usefulness as first step investigation, determining in vivo proof-of-concept from in vitro findings like immunoreactivity and examining the efficacy of radiotherapeutics on human tumor cells. However, apart from the benefits, the xenograft model has some significant disadvantages, such as the lack of organ/system microenvironment (except for orthotopic), the lack of immune system interaction with tumor cells, and cell lines likely differ significantly from the paternal source (tumor).

It is worth remembering that Rituximab, as a chimeric antibody including the variable region of the mouse immunoglobulin with human IgG1 heavy chain, is specific for and binds to human CD20 but does not bind to mouse or rat CD20.[76,77] At the same time, it does not react with CD20 on the mouse and rat lymphocytes.[78] Therefore, studies in healthy animals will not give a complete answer as to how the number of chelators will affect the biological activity of radiolabeled Rituximab (ability to depletion B lymphocytes), but only provide an answer concerning the pharmacokinetics of the obtained radioconjugates. Nevertheless, researchers could obtain information on how an increase of c/a, resulting in a higher molar activity (MA), affects its binding in nontarget organs, such as the liver. The liver is well-known to trapped mAb during its first pass effect by high-affinity low-capacity binding sites. Those studies, using healthy animals, can also help set up the clearance speed and plasma concentration.

Additional verification of the thesis given at the beginning of this article is the comparative study of the physiological distribution of radiolabeled Rituximab. Only some of the literature reports presented in Table 2 contain information about the relationship between the amount of attached chelator, molar activity, immunoreactivity, and organ distribution. Additionally, the test methods applied in the literature are diverse, such as different mice strains, cell lines, or radiopharmaceutical doses, so drawing a general conclusion is challenging. Therefore, we pulled out some commonalities between the research groups to compare data across studies and minimize variation. Those are the intravenous administration of the preparation, similar end points (24 h after administration), subcutaneous tumor induction, and in vitro preceded in vivo studies. To establish whether the number of conjugated chelators to mAb against CD-20 significantly affects physio-

https://doi.org/10.1021/acs.jmedchem.1c02044
J. Med. Chem. 2022, 65, 6419−6430

Table 3. Physiological distribution of Radiolabelled Rituximab in Different Healthy Murine Models[a]

	DOTA:mAb ratio (initial DOTA:mAb ratio)							
	1.6 (5:1) DOTA-NHS	2 (6:1) p-NCS-Bz-DOTA	6.4 (10:1) DOTA-NHS	5.6 (10:1) p-NCS-Bz-DOTA	8 (10:1) p-NCS-Bz-DOTA	4 (20:1) p-NCS-Bz-DOTA	11 (50:1) DOTA-NHS	17 (100:1) DOTA-NHS
mice	normal	BALB/c	normal	Swiss	BALB/c	BALB/c	normal	BALB/c
ref	30	73	30	43[b]	75	38	30	75
blood	10.1 ± 0.1	14 ± 3	10.07 ± 1.03	12.3 ± 1.9	17.4 ± 2.8	10.5 ± 1.34	0.11 ± 0.32	21.3 ± 2.4
lung	5.0 ± 1.3	6 ± 2	5.46 ± 0.63	16.3 ± 4.8	10.4 ± 2.5	8.92 ± 0.13	1.23 ± 0.32	12.2 ± 0.7
heart	5.0 ± 1.3	n.d.[c]	3.73 ± 1.05	14.3 ± 1.3	n.d.[c]	5.71 ± 1.23	0.71 ± 0.20	n.d.[c]
liver	9.2 ± 3.6	5 ± 2	14.62 ± 2.14	3.3 ± 4.7	14.1 ± 2.3	19.3 ± 3.3	44.83 ± 2.58	11.8 ± 0.8
stomach	0.8 ± 0.1	n.d.[c]	0.65 ± 0.11	1.3 ± 0.0	n.d.[c]	1.71 ± 0.60	0.18 ± 0.16	n.d.[c]
spleen	3.44 ± 0.35	5 ± 3	8.62 ± 1.02	19.9 ± 2.6	10.9 ± 0.5	9.34 ± 1.49	7.99 ± 0.31	11.3 ± 2.5
kidneys	3.3 ± 0.5	5 ± 2	4.37 ± 0.89	15.6 ± 1.3	6.2 ± 0.2	8.2 ± 1.9	1.26 ± 0.26	7.5 ± 0.0
bone	1.4 ± 0.1	1.7 ± 0.7	3.60 ± 1.20	n.d.[c]	6.0 ± 2.0	5.13 ± 0.17	2.05 ± 1.05	2.7 ± 0.4
liver/blood	0.91	0.35	1.44	2.78	0.81	1.83	407.3	0.55
spleen/blood	0.34	0.35	0.85	1.62	0.62	0.89	72.6	0.53
kidneys/blood	0.33	0.35	0.42	1.27	0.35	0.78	11.45	0.35

[a]Data collected 24 h after intravenous administration (%ID g^{-1}, mean ± SD). [b]Data calculated based on figure in the publication. [c]n.d., no data.

Table 4. Physiological Distribution of Radiolabelled Rituximab in Different Xenograft Murine Models[a]

	DOTA:mAb ratio (initial DOTA:mAb ratio)			
	3 (10:1) NCS-DTPA	4 (10:1) p-NCS-Bz-DOTA	17 (100:1) DOTA-NHS	2 (6:1) p-NCS-Bz-DOTA
ref	40	41	41	73[c]
MA [GBq/mcmol]	53.2−79	47.5	47.5	43
mice	SCIDE	BALB/c Nude	BALB/c Nude	BALB/c Nude
blood	22.6 ± 4.4	8.9 ± 3.2	13.0 ± 1.7	12.2
lung	8.3 ± 1.2	4.6 ± 1.1	6.0 ± 0.2	4.7
heart	4.3 ± 0.5	n.d.[b]	n.d.[b]	3.5
liver	12.7 ± 1.4	10.8 ± 2.0	10.2 ± 1.7	5.6
spleen	15.1 ± 2.8	19.2 ± 10.8	28.7 ± 4.1	3.5
stomach	1.3 ± 0.4	n.d.[b]	n.d.[b]	0.7
kidneys	11.6 ± 0.4	4.4 ± 0.7	4.6 ± 1.1	4.3
bone	0.4 ± 0.15	4.9 ± 0.6	6.3 ± 2.3	1.5
tumor	9.1 ± 1.5	7.4 ± 1.4	7.3 ± 1.7	5.2
tumor/blood	0.40	0.83	0.56	0.43
tumor/liver	0.72	0.68	0.72	0.92
tumor/spleen	0.60	0.39	0.25	1.49
tumor/kidneys	0.78	1.61	1.59	1.2

[a]Data collected 24 h after intravenous administration (%ID g^{-1}, mean ± SD). [b]n.d., no data. [c]Data calculated based on the figure in the publication.

logical distribution, we decided to use the organ-to-blood and tumor-to-organ ratio rather than the absolute value of %ID g^{-1} of organs/tissue and tumor. The specific data concerning the uptake of radiolabeled Rituximab from selected publications (murine model) are given in Tables 3 and 4.

Nevertheless, we were also able to draw conclusions from research using rats as an animal model. The studies performed by Yousefnia et al.[69] and Gholipour et al.[36] have shown similar observations, although they used different DOTA chelators and the initial molar ratio of DOTA:mAb for conjugation (p-NCS-Bz-DOTA, 10:1 and DOTA-NHS, 1:1; respectively). High uptake in the liver, spleen, and other reticuloendothelial organs was observed due to the depletion of circulating B cells occurring rapidly after administration of radioimmunoconjugate. In the liver, the uptake of radio-labeled antibody decreased after 24 h but began to increase after 48 h due to secondary accumulation of released $^{90}Y/^{177}Lu$ ions due to metabolic degradation of the radio-labeled antibody. Interestingly, Bahrami-Samani A. et al.[71] reported a comparable result. The authors observed reabsorption of liver metabolites of [^{153}Sm]Sm-DTPA-Rituximab after 48 h with simultaneous increase of the whole body background. In addition, Gholipour et al. showed that faster clearance of radioactivity from the bloodstream was observed with the initial injection of unlabeled Rituximab (250 μg m-2) due to the blocking by cold Rituximab of positive CD-20 binding sites on B-lymphocytes in the circulation and spleen.[36]

More information describing our thesis comes from the physiological distribution of radiolabeled Rituximab in murine models. During the literature review, we came across only one publication (listed in Table 3,[30]) describing the effect of the number of p-NCS-Bz-DOTA chelators on the pharmacokinetics and immunoreactivity of radiolabeled Rituximab and two other publications based on anti-L1-CAM antibody chCE7.[79,80] However, the results of Guleria et al.[30] regarding DOTA-Rituximab with 11 chelators should not be considered due to the very poor serum stability of the conjugate (radiochemical yield <70% and <3 0% at 48 and 72 h, respectively). Therefore, an investigation of serum stability is performed to assess potential degradation/modification of the radioimminoconjugates by enzymes in plasma. In Table 3, four publications[29,38,43,74] describing a biodistribution study are based on Rituximab coupled with a p-SCN-Bz-DOTA chelator. Therefore, a null

https://doi.org/10.1021/acs.jmedchem.1c02044
J. Med. Chem. 2022, 65, 6419−6430

hypothesis should be separated for distribution in healthy mice claim that there is no statistically significant correlation between target-to-blood and for distribution in xenograft mice model claim that there is no statistically significant correlation between tumor-to-target ratio for considered conjugates. For statistical analysis, two-way ANOVA was performed using GraphPad Prism version 8.00 for Windows. In all cases, a p-value of <0.05 was considered statistically significant.

On the basis of the statistical analysis and the obtained p-value, we can conclude that in the group of healthy mice, there is a statistically significant influence of the number of attached chelators on the organ-to-blood ratio ($p < 0.05$, Figure 3A),

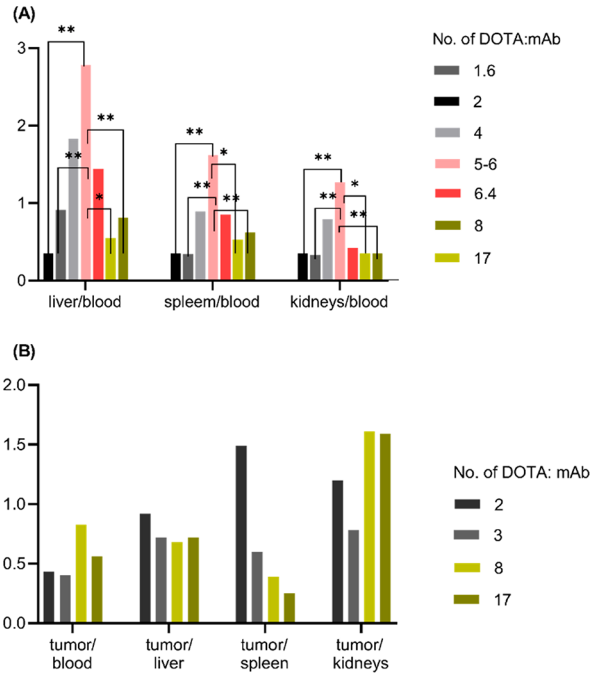

Figure 3. Graphical presentation of target-to-blood (A) and tumor-to-target ratios (B) for conjugates with different numbers of chelators conjugated to Rituximab. Data was collected 24 h after intravenous administration—analyses based on data listed in Tables 3 and 4, respectively.

whereas in the group of xenografted mice there are no statistically significant differences ($p > 0.05$), Figure 3B. Although a statistically significant influence was observed, it cannot be said that this relation is positively linear for all observations. A linear increase in the organ-to-blood ratio was observed until the number of attached chelators reached about six, and then a decrease in the organ-to-blood ratio was observed. This finding is most likely due to the slower elimination of conjugates from the blood and increased hydrophilic moieties in the antibody structure. Guleria et al.[30] pointed out that the conjugate's hydrophilic character may interfere with the bioaffinity of Rituximab, which is responsible for identifying and binding with the antigen receptors. However, this is in contrast to that Rituximab does not bind to mouse CD20.[78]

The general observations from all collected cases concerning pharmacokinetics are as follows: the highest activity concentration was initially in blood and the liver. The blood activity level at 24 h p.i. was similar for all examined conjugates and did not depend on the number of conjugated DOTA. No significant differences of accumulation in organs/tissue like liver and blood were observed. The only organ that can indicate the effect of the chelator amount on the change in the pharmacokinetics of the conjugate is the spleen. The bone uptake between 2 to 8% ID g^{-1} was noticed and depended on the in vivo stability of the radioconjugate. This is somewhat contrary to the trend observed by Guleria et al., where Rituximab was chemically functionalized with 5, 10, and 50 p-NCS-Bz-DOTA chelators. They published results showing that an increased number of hydrophilic p-NCS-Bz-DOTA moieties in the antibody structure will increase the conjugate's hydrophilic character and interfere with Rituximab's bioaffinity. The different pharmacokinetic behavior of the radioconjugates supported this observation. However, it should be noted that p-NCS-Bz-DOTA-Rituximab with 11 chelators should not be considered due to the authors' very poor stability of the conjugate claim.[30]

In all studies (rat and mice models), significant clearance of radioactive Rituximab took place through the hepatobiliary pathway, which is well established for monoclonal antibodies. The in vivo stability of radiolabeled mAb is indicated by low bone uptake considering the high affinity of free $^{177}Lu/^{90}Y$ to bone tissue.[81] The distribution of antibodies is restricted primarily to plasma and extracellular fluids and is concentrated at tissues expressing the target antigen, especially in tumors in xenograft mouse studies.[82,83]

CONCLUSIONS

The purpose of this review was to answer whether and how the number of bifunctional chelators conjugated to a mAb against CD-20 affects the biological activity of its radio-labeled counterpart.

The research reviewed clearly shows that the increased number of DOTA chelators attached to Rituximab affects the molecular activity and decreases the immunoreactivity of modified monoclonal antibody (statistically significant - $p = 0.0074$, low negative correlation; Pearson's correlation equals 0.4362). Furthermore, mAbs are not robust when higher conjugate ratios of chelator are used, and most of the antibody's immunoreactivity is lost, which renders such conjugates not useful in patients.

However, the results show large variations between research groups mainly caused by applying different methods for the determination of c/a or immunoreactivity and imperfections and limitations of these methods. Along with those observations, one would expect a correlation between c/a and pharmacokinetics or tumor uptake in vivo. In the group of healthy mice, there is a statistically significant influence of the number of attached chelators on the organ-to-blood ratio ($p < 0.05$), which relate to the metabolism and clearance of the counterpart with changing hydrophilicity, whereas, in the group of xenografted mice, there are no statistically significant differences ($p > 0.05$) in the tumor-to-organ ratio. In our opinion, this observation is correlated with similar molar activity injected into xenografted mice and is not dependent on the chelator to mAb ratio.

We want to underline that our conclusion concerning biological studies is based on selected results: the intravenous administration of the preparation, ex vivo biodistribution at 24 h after administration, subcutaneous tumor induction, and in vitro preceded in vivo studies. Therefore, to better understand the chelator's influence on the immunoconjugate's biological activity, it would be necessary to compare the results obtained in different laboratories but working according to the same standard procedures. Moreover, it should be remembered that in vivo studies on Rituximab labeled with lutetium-177 or yttrium-

https://doi.org/10.1021/acs.jmedchem.1c02044
J. Med. Chem. 2022, 65, 6419−6430

90 should be conducted for at least 4−6 days, taking into account the half-life of the radioisotopes. Then the comparison would be more plausible.

AUTHOR INFORMATION

Corresponding Authors

Urszula Karczmarczyk − *National Centre for Nuclear Research, Radioisotope Centre POLATOM, Otwock 05-400, Poland*; orcid.org/0000-0001-7841-3946; Phone: +48 22 273 19 26; Email: urszula.karczmarczyk@polatom.pl

Agnieszka Sawicka − *National Centre for Nuclear Research, Radioisotope Centre POLATOM, Otwock 05-400, Poland*; Phone: +48 22 273 19 20; Email: Agnieszka.sawicka@polatom.pl

Authors

Piotr Garnuszek − *National Centre for Nuclear Research, Radioisotope Centre POLATOM, Otwock 05-400, Poland*

Michał Maurin − *National Centre for Nuclear Research, Radioisotope Centre POLATOM, Otwock 05-400, Poland*

Wioletta Wojdowska − *National Centre for Nuclear Research, Radioisotope Centre POLATOM, Otwock 05-400, Poland*

Complete contact information is available at: https://pubs.acs.org/10.1021/acs.jmedchem.1c02044

Author Contributions

Conceptualization, U.K., W.W.; methodology, U.K., M.M., W.W., A.S., and P.G., writing−original draft preparation, U.K., A.S., and M.M.; writing−review and editing, U.K., M.M., P.G., A.S., and W.W.; in vitro and in vivo studies, W.W. and U.K., critical analysis and correction of the manuscript, P.G., U.K., and M.M. All authors have given approval to the final version of the manuscript.

Funding

This research received no external funding.

Notes

The authors declare no competing financial interest.

Biographies

Urszula Karczmarczyk received a PhD degree in biotechnology in 2003 from Warsaw University of Technology, Poland. She has been a research scientist in the radiopharmaceutical field for over 20 years and has held the Head of Preclinical Laboratory position at National Centre for Nuclear Research, Radioisotope Centre POLATOM since 2011. She conducted research on radiolabeling and the biological activity of IL-2 as a potential scintigraphy agent for unspecific inflammatory process detection in the Laboratory of Professor Albert Signore at "La Sapienza" University, Italy, in 2007. She serves as reviewer and cochair of the ESMI Conference, and she is a member of the Polish Laboratory Animal Science Association, European Society of Molecular Imaging and Polish Society of Nuclear Medicine. Co-author of three patents and 31 publications.

Agnieszka Sawicka received an MSc in Biochemistry from Lodz University in 2001. Subsequently, she researched lipoprotein metabolism and inflammatory mediators at University Clinic Großhadern in Munich. Later on, as part of her PhD, she was engaged in research on chromosomal alteration and DNA repair after oxidative damage at the University of Munich. In parallel, she worked in Contract Research Organizations in toxicological research. Finally, she earned a PhD in human biology in 2010 at the Ludwig Maximilian University of Munich, Faculty of Medicine. Currently, she works as a scientist in the National Centre for Nuclear Research, Radioisotope Centre POLATOM. She is responsible for planning and coordinating toxicological studies and is involved in few research projects on new radiopharmaceuticals, analytical methods, and registrations procedures.

Michał Maurin received an MSc. degree in Chemical technology in 2002 at Warsaw University of Technology, Poland. Since then, He is a research scientist in the field of radiopharmacy. His main field of interest is developing new radiopharmaceuticals, assessing radiopharmaceuticals' quality, and the comprehensive preclinical studies. He is the coauthor of over 25 articles in radiopharmacy and over 70 conference communications. Currently, he works at the National Centre for Nuclear Research, Radioisotope Centre POLATOM, and is the Head of the API production department. He is a member of the Polish Society of Nuclear Medicine and the European Society of Nuclear Medicine.

Piotr Garnuszek, PhD, DSc in pharmaceutical sciences, is an Associate Professor at the NCBJ, Radioisotope Centre POLATOM and Head of the R&D Department. He is a member of the expert Group 14 − Radioactive Compounds of the European Pharmacopoeia. His main field of interest is developing new radiopharmaceuticals, assessing radiopharmaceuticals' quality and the comprehensive preclinical studies. Co-author of 65 publications. *Pharmaceuticals* **2021**, *14*, 1107, *Int. J. Mol. Sci.* **2021**, *22*, 5702, *Front. Med.* **2021**, *8*, 647379, *EJNMMI Radiopharm. Chem.* **2021**, *6*, 19, *Arch. Med. Sci.* **2021**, *17*(3), 38−842, *Tetrahedron* **2021**, *84*, 132018, *Int. J. Mol. Sci.* **2021**, *22*, 2731, *Pharmaceuticals* **2021**, *14*, 19, *Nucl. Med. Biol.* **2021**, *93*, 63−73, *Cancer. Biotherapy Radiopharm.* **2020**, *35*(8), 558−562, *Spectrochim. Acta Part A: Mol. Biomol. Spectrosc.* **2020**, *231*, 117791, *Nucl. Med. Rev.* **2019**, *22*(2),1−4, *Appl. Radiat. Isotop.* **2019**, *151*, 140−144, *Pol. Arch. Intern. Med.* **2018**, *128*(12), 791−795, *EJNMMI Res.* **2018**, *8*, 33

Wioletta Wojdowska. She received a PhD degree in biotechnology in 2007 from Technical University at Lodz. Currently, she is the Head of the Radiopharmaceutical Laboratory at the National Centre for Nuclear Research. She has over 15 years of work experience in radioisotopes and radiopharmaceutical research, focusing on the development of radiopharmaceuticals for clinical use. She is a Member of the Polish Society of Nuclear Medicine and a project partner in the International Atomic Energy Agency (IAEA) coordinated research programs.

ABBREVIATIONS USED

BCA, bifunctional chelators or bifunctional chelating agents; B_{max}, maximum receptor density; DOTA-NHS, N-hydroxysulfosuccinimidy; DTPA, polyaminocarboxylic acid; FDA, Food and Drug Administration; ID, injected dose; IRF, immunoreactive fraction; K_D, binging affinity; MA, molar activity; mAb, monoclonal antibody; mcg, microgram; mcmol, micromole; MW, molecular weight; NHL, non-Hodgkin's lymphoma; pI, isoelectric point; p-NCS-Bz-DOTA, 1,4,7,10-tetraazacyclododecane-N,N',N',N'-1,4,7,10-tetraacetic acid; RIT, radioimmunotherapy; RSD, relative standard deviation; SD, standard deviation; SE HPLC, size-exclusion high-performance liquid chromatography; EM, tumor microenvironment

REFERENCES

(1) Zahavi, D.; Weiner, L. Monoclonal Antibodies in Cancer Therapy. *Antibodies* **2020**, *9* (3), 34.

(2) Seebacher, N. A.; Stacy, A. E.; Porter, G. M.; Merlot, A. M. Clinical Development of Targeted and Immune Based Anti-Cancer Therapies. *J. Exp. Clin. Cancer Res.* **2019**, *38* (1), 156.

(3) Chiavenna, S. M.; Jaworski, J. P.; Vendrell, A. State of the Art in Anti-Cancer MAbs. *J. Biomed. Sci.* **2017**, *24* (1), 15.

(4) Zhao, X.; Subramanian, S. Oncogenic Pathways That Affect Antitumor Immune Response and Immune Checkpoint Blockade Therapy. *Pharmacol. Ther.* **2018**, *181*, 76−84.
(5) Ludwig, D. L.; Pereira, D. S.; Zhu, Z.; Hicklin, D. J.; Bohlen, P. Monoclonal Antibody Therapeutics and Apoptosis. *Oncogene* **2003**, *22* (56), 9097−9106.
(6) Hicklin, D. J.; Witte, L.; Zhu, Z.; Liao, F.; Wu, Y.; Li, Y.; Bohlen, P. Monoclonal Antibody Strategies to Block Angiogenesis. *Drug Discovery Today* **2001**, *6* (10), 517−528.
(7) Jiang, L.; Li, N. B-Cell Non-Hodgkin Lymphoma: Importance of Angiogenesis and Antiangiogenic Therapy. *Angiogenesis* **2020**, *23* (4), 515−529.
(8) Kimiz-Gebologlu, I.; Gulce-Iz, S.; Biray-Avci, C. Monoclonal Antibodies in Cancer Immunotherapy. *Mol. Biol. Rep.* **2018**, *45* (6), 2935−2940.
(9) Lacey, D. L.; Boyle, W. J.; Simonet, W. S.; Kostenuik, P. J.; Dougall, W. C.; Sullivan, J. K.; Martin, J. S.; Dansey, R. Bench to Bedside: Elucidation of the OPG−RANK−RANKL Pathway and the Development of Denosumab. *Nat. Rev. Drug Discovery* **2012**, *11* (5), 401−419.
(10) Goldmacher, V. S.; Kovtun, Y. V. Antibody−Drug Conjugates: Using Monoclonal Antibodies for Delivery of Cytotoxic Payloads to Cancer Cells. *Ther. Delivery* **2011**, *2* (3), 397−416.
(11) Rituxan (Rituximab)—First New Drug for Non-Hodgkin's Lymphoma in a Decade Receives FDA Clearance for Marketing https://www.drugs.com/history/rituxan.html.
(12) Witzig, T. Radioimmunotherapy for Patients with Relapsed B-Cell Non-Hodgkin Lymphoma. *Cancer Chemother. Pharmacol.* **2001**, *48* (0), S91−S95.
(13) Alcindor, T.; Witzig, T. E. Radioimmunotherapy with Yttrium-90 Ibritumomab Tiuxetan for Patients with Relapsed Cd20+ B-Cell Non-Hodgkin's Lymphoma. *Curr. Treat. Options Oncol.* **2002**, *3* (4), 275−282.
(14) Wikipedia. Wikipedia, CD20 (accessed March 1, 2022).
(15) Postema, E. J.; Boerman, O. C.; Oyen, W. J.; Raemaekers, J. M.; Corstens, F. H. Radioimmunotherapy of B-Cell Non-Hodgkin's Lymphoma. *Eur. J. Nucl. Med.* **2001**, *28* (11), 1725−1735.
(16) DeNardo, G. L. Treatment of Non-Hodgkin's Lymphoma (NHL) with Radiolabeled Antibodies (MAbs). *Semin. Nucl. Med.* **2005**, *35* (3), 202−211.
(17) Forero, A.; Lobuglio, A. F. History of Antibody Therapy for Non-Hodgkin's Lymphoma. *Semin. Oncol.* **2003**, *30* (6), 1−5.
(18) Oyen, W. J.; Postema, E. J.; Corstens, F. H.; Boerman, O. C.; Koppe, M. J. Radionuclide Therapy of Cancer with Radiolabeled Antibodies. *Anticancer Agents Med. Chem.* **2007**, *7* (3), 335−343.
(19) Pham, D. T.; Kaspersen, F. M.; Bos, E. S. Electrophoretic Method for the Quantitative Determination of a Benzyl-DTPA Ligand in DTPA Monoclonal Antibody Conjugates. *Bioconjugate Chem.* **1995**, *6* (3), 313−315.
(20) Kukis, D. L.; DeNardo, G. L.; DeNardo, S. J.; Mirick, G. R.; Miers, L. A.; Greiner, D. P.; Meares, C. F. Effect of the Extent of Chelate Substitution on the Immunoreactivity and Biodistribution of 2IT-BAT-Lym-1 Immunoconjugates. *Cancer Res.* **1995**, *55* (4), 878−884.
(21) Knogler, K.; Grünberg, J.; Zimmermann, K.; Cohrs, S.; Honer, M.; Ametamey, S.; Altevogt, P.; Fogel, M.; Schubiger, P. A.; Novak-Hofer, I. Copper-67 Radioimmunotherapy and Growth Inhibition by Anti-L1-Cell Adhesion Molecule Monoclonal Antibodies in a Therapy Model of Ovarian Cancer Metastasis. *Clin. Cancer Res. Off. J. Am. Assoc. Cancer Res.* **2007**, *13* (2), 603−611.
(22) Byegård, J.; Skarnemark, G.; Skålberg, M. The Stability of Some Metal EDTA, DTPA and DOTA Complexes: Application as Tracers in Groundwater Studies. *J. Radioanal. Nucl. Chem.* **1999**, *241* (2), 281−290.
(23) Stimmel, J. B.; Kull, F. C. Samarium-153 and Lutetium-177 Chelation Properties of Selected Macrocyclic and Acyclic Ligands. *Nucl. Med. Biol.* **1998**, *25* (2), 117−125.
(24) Cramer, F.; Kampe, W. Inclusion Compounds. XVII. 1 Catalysis of Decarboxylation by Cyclodextrins. A Model Reaction for the Mechanism of Enzymes. *J. Am. Chem. Soc.* **1965**, *87* (5), 1115−1120.
(25) Roselli, M.; Schlom, J.; Gansow, O. A.; Brechbiel, M. W.; Mirzadeh, S.; Pippin, C. G.; Milenic, D. E.; Colcher, D. Comparative Biodistribution Studies of DTPA-Derivative Bifunctional Chelates for Radiometal Labeled Monoclonal Antibodies. *Int. J. Rad. Appl. Instrum. B* **1991**, *18* (4), 389−394.
(26) Camera, L.; Kinuya, S.; Garmestani, K.; Wu, C.; Brechbiel, M. W.; Pai, L. H.; McMurry, T. J.; Gansow, O. A.; Pastan, I.; Paik, C. H. Evaluation of the Serum Stability and in Vivo Biodistribution of CHX-DTPA and Other Ligands for Yttrium Labeling of Monoclonal Antibodies. *J. Nucl. Med. Off. Publ. Soc. Nucl. Med.* **1994**, *35* (5), 882−889.
(27) Brechbiel, M. W.; Gansow, O. A.; Atcher, R. W.; Schlom, J.; Esteban, J.; Simpson, D.; Colcher, D. Synthesis of 1-(p-Isothiocyanatobenzyl) Derivatives of DTPA and EDTA. Antibody Labeling and Tumor-Imaging Studies. *Inorg. Chem.* **1986**, *25* (16), 2772−2781.
(28) Banerjee, S.; Pillai, M. R. A.; Knapp, F. F. R. Lutetium-177 Therapeutic Radiopharmaceuticals: Linking Chemistry, Radiochemistry, and Practical Applications. *Chem. Rev.* **2015**, *115* (8), 2934−2974.
(29) Wojdowska, W.; Karczmarczyk, U.; Balog, L.; Sawicka, A.; Pösténvi, Z.; Kovács-Haász, V.; Polyák, A.; Laszuk, E.; Mikołajczak, R.; Garnuszek, P. Impact of DOTA-Chelators on the Antitumor Activity of 177 Lu-DOTA-Rituximab Preparations in Lymphoma Tumor-Bearing Mice. *Cancer Biother. Radiopharm.* **2020**, *35* (8), 558−562.
(30) Guleria, M.; Das, T.; Kumar, C.; Sharma, R.; Amirdhanayagam, J.; Sarma, H. D.; Dash, A. Effect of Number of Bifunctional Chelating Agents on the Pharmacokinetics and Immunoreactivity of 177Lu-Labeled Rituximab: A Systemic Study. *Anticancer Agents Med. Chem.* **2018**, *18* (1), 146−153.
(31) Liu, Y.-F.; Wu, C.-C. Radiolabeling of Monoclonal Antibodies with Metal Chelates. *Pure Appl. Chem.* **1991**, *63* (3), 427−463.
(32) Pippin, C. G.; McMurry, T. J.; Brechbiel, M. W.; McDonald, M.; Lambrecht, R.; Milenic, D.; Roselli, M.; Colcher, D.; Gansow, O. A. Lead(II) Complexes of 1,4,7,10-Tetraazacyclododecane-N,N′,N″,N‴-Tetraacetate: Solution Chemistry and Application to Tumor Localization with 203Pb Labeled Monoclonal Antibodies. *Inorg. Chim. Acta* **1995**, *239* (1−2), 43−51.
(33) Dadachova, E.; Chappell, L. L.; Brechbiel, M. W. Spectrophotometric Method for Determination of Bifunctional Macrocyclic Ligands in Macrocyclic Ligand−Protein Conjugates. *Nucl. Med. Biol.* **1999**, *26* (8), 977−982.
(34) Brady, E. D.; Chong, H.-S.; Milenic, D. E.; Brechbiel, M. W. Development of a Spectroscopic Assay for Bifunctional Ligand-Protein Conjugates Based on Copper. *Nucl. Med. Biol.* **2004**, *31* (6), 795−802.
(35) Pippin, C. G.; Parker, T. A.; McMurry, T. J.; Brechbiel, M. W. Spectrophotometric Method for the Determination of a Bifunctional DTPA Ligand in DTPA-Monoclonal Antibody Conjugates. *Bioconjugate Chem.* **1992**, *3* (4), 342−345.
(36) Gholipour, N.; Jalilian, A. R.; Khalaj, A.; Johari-Daha, F.; Yavari, K.; Sabzevari, O.; Khanchi, A. R.; Akhlaghi, M. Preparation and Radiolabeling of a Lyophilized (Kit) Formulation of DOTA-Rituximab with 90Y and 111In for Domestic Radioimmunotherapy and Radioscintigraphy of Non-Hodgkin's Lymphoma. *DARU J. Pharm. Sci.* **2014**, *22* (1), 58.
(37) Suman, S. K.; Kameswaran, M.; Pandey, U.; Sarma, H. D.; Dash, A. Preparation and Preliminary Bioevaluation Studies of 68 Ga-NOTA-Rituximab Fragments as Radioimmunoscintigraphic Agents for Non-Hodgkin Lymphoma. *J. Label. Compd. Radiopharm.* **2019**, *62* (12), 850−859.
(38) Johari-Doha, F.; Rahmani, S.; Rasaneh, S.; Sheikholislam, Z.; Shahhosseini, S. Development of DOTA-Rituximab Kit Formulation to Be Labeled with 90Y for Radioimmunotherapy of B-Cell Non-Hodgkin Lymphoma.*Iran. J. Pharm. Res.* **2017**, *16* (2) DOI: 10.22037/ijpr.2017.2109.
(39) Johari Daha, F.; Rasaneh, S.; Salehi Zahabi, S. Preparation of ^{177}Lu-Rituximab and Comparison with ^{131}I-Rituximab Radiolabeled with Chloramine-T Method. *J. Clin. Res. Paramed. Sci.* **2018**, DOI: 10.5812/jcrps.87181, In Press.
(40) Kameswaran, M.; Pandey, U.; Dhakan, C.; Pathak, K.; Gota, V.; Vimalnath, K. V.; Dash, A.; Samuel, G. Synthesis and Preclinical

Evaluation of 177 Lu-CHX-A″-DTPA-Rituximab as a Radioimmunotherapeutic Agent for Non-Hodgkin's Lymphoma. Cancer Biother. *Radiopharm* **2015**, *30* (6), 240−246.
(41) Karczmarczyk, U.; Wojdowska, W.; Mikolajczak, R.; Maurin, M.; Laszuk, E.; Garnuszek, P. Influence of DOTA Chelators on Radiochemical Purity and Biodistribution of 177Lu- and 90Y-Rituximab in Xenografted Mic. Iran. *J. Pharm. Res.* **2018**, *17* (4), 1201−1208.
(42) Forrer, F.; Chen, J.; Fani, M.; Powell, P.; Lohri, A.; Müller-Brand, J.; Moldenhauer, G.; Maecke, H. R. In Vitro Characterization of 177Lu-Radiolabelled Chimeric Anti-CD20 Monoclonal Antibody and a Preliminary Dosimetry Study. *Eur. J. Nucl. Med. Mol. Imaging* **2009**, *36* (9), 1443−1452.
(43) Kameswaran, M.; Pandey, U.; Dash, A.; Samuel, G.; Venkatesh, M. Preparation & in Vitro Evaluation of ^{90}Y-DOTA-Rituximab. *Indian J. Med. Res.* **2016**, *143* (1), 57.
(44) definicja Immunoreactive | Definition of Immunoreactive by Merriam-Webster.
(45) Lindmo, T.; Boven, E.; Cuttitta, F.; Fedorko, J.; Bunn, P. A. Determination of the Immunoreactive Function of Radiolabeled Monoclonal Antibodies by Linear Extrapolation to Binding at Infinite Antigen Excess. *J. Immunol. Methods* **1984**, *72* (1), 77−89.
(46) Dux, R.; Kindler-Röhrborn, A.; Lennartz, K.; Rajewsky, M. F. Determination of Immunoreactive Fraction and Kinetic Parameters of a Radiolabeled Monoclonal Antibody in the Absence of Antigen Excess. *J. Immunol. Methods* **1991**, *144* (2), 175−183.
(47) Mattes, M. J. Limitations of the Lindmo Method in Determining Antibody Immunoreactivity. *Int. J. Cancer* **1995**, *61* (2), 286−288.
(48) Konishi, S.; Hamacher, K.; Vallabhajosula, S.; Kothari, P.; Bastidas, D.; Bander, N.; Goldsmith, S. Determination of Immunoreactive Fraction of Radiolabeled Monoclonal Antibodies: What Is an Appropriate Method? Cancer Biother. *Radiopharm* **2004**, *19* (6), 706−715.
(49) Yin, O.; Narula, J.; Nossiff, N.; An Khaw, B. Correlation of Immunoreactivity and Polymer Formation to DTPA Modification of a Monoclonal Antibody. *Int. J. Rad. Appl. Instrum. B* **1991**, *18* (8), 859−864.
(50) Sinkule, J. A.; Rosen, S. T.; Radosevich, J. A. Monoclonal Antibody 44−3A6 Doxorubicin Immunoconjugates: Comparative in Vitro Anti-Tumor Efficacy of Different Conjugation Methods. *Tumor Biol.* **1991**, *12* (4), 198−206.
(51) Reilly, R.; Lee, N.; Houle, S.; Law, J.; Marks, A. In Vitro Stability of EDTA and DTPA Immunoconjugates of Monoclonal Antibody 2G3 Labeled with Indium-111. *Int. J. Rad. Appl. Instrum. [A]* **1992**, *43* (8), 961−967.
(52) Slinkin, M. A.; Klibanov, A. L.; Khaw, B. A.; Torchilin, V. P. Succinylated Polylysine as a Possible Link between an Antibody Molecule and Deferoxamine. *Bioconjugate Chem.* **1990**, *1* (4), 291−295.
(53) Sawicka, A.; Wojdowska, W.; Karczmarczyk, U.; Maurin, M.; Byszewska-Szpocińska, E.; Garnuszek, P.; Mikołajczak, R. Immunoreaktywność przeciwciała anty-CD20 chelatowanego DOTA do znakowania ^{90}Y i ^{177}Lu; *Nucl. Med. Rev.: Lublin*, **2014**, *17*.
(54) Thakral, P.; Singla, S.; Yadav, M. P.; Vasisht, A.; Sharma, A.; Gupta, S. K.; Bal, C. S.; Snehlata; Malhotra, A. An Approach for Conjugation of (^{177})Lu- DOTA-SCN- Rituximab (BioSim) & Its Evaluation for Radioimmunotherapy of Relapsed & Refractory B-Cell Non Hodgkins Lymphoma Patients. *Indian J. Med. Res.* **2014**, *139* (4), 544−554.
(55) Wojdowska, W.; Karczmarczyk, U.; Maurin, M.; Garnuszek, P.; Mikołajczak, R. Standardization of Procedures for the Preparation of ^{177}Lu- and ^{90}Y-labeled DOTA-Rituximab Based on the Freeze-dried Kit Formulation. *CRP* **2015**, *8* (1), 62−68.
(56) Hau, J. Animal Models for Human Diseases. In *Sourcebook of Models for Biomedical Research*; Conn, P. M., Ed.; Humana Press: Totowa, NJ, 2008; pp 3−8 DOI: 10.1007/978-1-59745-285-4_1.
(57) Daydé, D.; Ternant, D.; Ohresser, M.; Lerondel, S.; Pesnel, S.; Watier, H.; Le Pape, A.; Bardos, P.; Paintaud, G.; Cartron, G. Tumor Burden Influences Exposure and Response to Rituximab: Pharmacokinetic-Pharmacodynamic Modeling Using a Syngeneic Bioluminescent Murine Model Expressing Human CD20. *Blood* **2009**, *113* (16), 3765−3772.
(58) Cheadle, E. J.; Lipowska-Bhalla, G.; Dovedi, S. J.; Fagnano, E.; Klein, C.; Honeychurch, J.; Illidge, T. M. A TLR7 Agonist Enhances the Antitumor Efficacy of Obinutuzumab in Murine Lymphoma Models via NK Cells and CD4 T Cells. *Leukemia* **2017**, *31* (7), 1611−1621.
(59) Herting, F.; Friess, T.; Bader, S.; Muth, G.; Hölzlwimmer, G.; Rieder, N.; Umana, P.; Klein, C. Enhanced Anti-Tumor Activity of the Glycoengineered Type II CD20 Antibody Obinutuzumab (GA101) in Combination with Chemotherapy in Xenograft Models of Human Lymphoma. *Leuk. Lymphoma* **2014**, *55* (9), 2151−5160.
(60) Day, C.-P.; Merlino, G.; VanDyke, T. Preclinical Mouse Cancer Models: A Maze of Opportunities and Challenges. *Cell* **2015**, *163* (1), 39−53.
(61) Awasthi, A.; Ayello, J.; van de Ven, C.; Hovy, S.; Cairo, M. S. Obinutuzumab (GA101) Significantly Improves Survival In CD20 Positive Pre-B Cell Lymphoblastic Leukemia (Pre-B-ALL) Xenograft Models Compared To Rituximab (RTX): Potential Targeted Therapy In Patients With High Risk Pre-B-ALL. *Blood* **2013**, *122* (21), 3068−3068.
(62) Köberle, M.; Müller, K.; Kamprad, M.; Horn, F.; Scholz, M. Monitoring Disease Progression and Therapeutic Response in a Disseminated Tumor Model for Non-Hodgkin Lymphoma by Bioluminescence Imaging. *Mol. Imaging* **2015**, *14* (6), 00010.
(63) Kohnken, R.; Porcu, P.; Mishra, A. Overview of the Use of Murine Models in Leukemia and Lymphoma Research. *Front. Oncol.* **2017**, *7* DOI: 10.3389/fonc.2017.00022.
(64) Kopetz, S.; Lemos, R.; Powis, G. The Promise of Patient-Derived Xenografts: The Best Laid Plans of Mice and Men: Figure 1. *Clin. Cancer Res.* **2012**, *18* (19), 5160−5162.
(65) Macchiarini, F.; Manz, M. G.; Palucka, A. K.; Shultz, L. D. Humanized Mice. *J. Exp. Med.* **2005**, *202* (10), 1307−1311.
(66) Lee, E. K.; Joo, E. H.; Song, K.-A.; Choi, B.; Kim, M.; Kim, S.-H.; Kim, S. J.; Kang, M.-S. Effects of Lymphocyte Profile on Development of EBV-Induced Lymphoma Subtypes in Humanized Mice. *Proc. Natl. Acad. Sci. U. S. A.* **2015**, *112* (42), 13081−13086.
(67) Adams, J. M.; Harris, A. W.; Pinkert, C. A.; Corcoran, L. M.; Alexander, W. S.; Cory, S.; Palmiter, R. D.; Brinster, R. L. The C-Myc Oncogene Driven by Immunoglobulin Enhancers Induces Lymphoid Malignancy in Transgenic Mice. *Nature* **1985**, *318* (6046), 533−538.
(68) Egle, A.; Harris, A. W.; Bath, M. L.; O'Reilly, L.; Cory, S. VavP-Bcl2 Transgenic Mice Develop Follicular Lymphoma Preceded by Germinal Center Hyperplasia. *Blood* **2004**, *103* (6), 2276−2283.
(69) Yousefnia, H.; Radfar, E.; Jalilian, A. R.; Bahrami-Samani, A.; Shirvani-Arani, S.; Arbabi, A.; Ghannadi-Maragheh, M. Development of 177Lu-DOTA-Anti-CD20 for radioimmunotherapy. *J. Radioanal. Nucl. Chem.* **2011**, *287* (1), 199−209.
(70) 153Sm-DTPA-rituximab https://www.yumpu.com/en/document/read/22461082/development-of-153sm-dtpa-rituximab-for-radioimmunotherapy.
(71) Muldoon, L. L.; Lewin, S. J.; Dósa, E.; Kraemer, D. F.; Pagel, M. A.; Doolittle, N. D.; Neuwelt, E. A. Imaging and Therapy with Rituximab Anti-CD20 Immunotherapy in an Animal Model of Central Nervous System Lymphoma. *Clin. Cancer Res.* **2011**, *17* (8), 2207−2215.
(72) Jalilian, A. R.; Mirsadegh, L.; Haji-Hosseini, R.; Rajabifar, S.; Bolurinovin, F. Production and evaluation of (67 Ga)-DTPA-Rituximab. *Iran J. Radiat Res.* **2007**, *4* (4), 187−193.
(73) Audicio, P. F.; Castellano, G.; Tassano, M. R.; Rezzano, M. E.; Fernandez, M.; Riva, E.; Robles, A.; Cabral, P.; Balter, H.; Oliver, P. [177Lu]DOTA-Anti-CD20: Labeling and Pre-Clinical Studies. *Appl. Radiat. Isot.* **2011**, *69* (7), 924−928.
(74) Repetto-Llamazares, A. H. V.; Larsen, R. H.; Mollatt, C.; Lassmann, M.; Dahle, J. Biodistribution and Dosimetry of (177)Lu-Tetulomab, a New Radioimmunoconjugate for Treatment of Non-Hodgkin Lymphoma. *Curr. Radiopharm.* **2013**, *6* (1), 20−27.
(75) Wojdowska, W.; Karczmarczyk, U.; Maurin, M.; Sawicka, A.; Laszuk, E.; Garnuszek, P.; Mikołajczak, R. In Virto and in Vivo

https://doi.org/10.1021/acs.jmedchem.1c02044
J. Med. Chem. 2022, 65, 6419−6430

Investigations of ^{177}Lu and ^{90}Y Labeled DOTA(SCN)-Rituximab Radioimmunoconjugates. *Q J. Nucl. Med. Mol. Imaging* **2014**, *58* (2), 45.
(76) Maloney, D. G. Anti-CD20 antibody therapy for B-cell lymphomas. *N Engl J. Med.* **2012**, *366*, 2008−2016.
(77) Klein, C.; Lammens, A.; Schäfer, W.; Georges, G.; Schwaiger, M.; Mössner, E.; Hopfner, K. P.; Umaña, P.; Niederfellner, G. Epitope interactions of monoclonal antibodies targeting CD20 and their relationship to functional properties. *MAbs* **2013**, *5*, 22−33.
(78) Regal, J. F.; Laule, C. F.; Root, K. M.; Gilbert, J. F.; Fleming, S. D. Reply to ″Letter to the Editor: Importance of B cells in response to placental ischemia″. *Am. J. Physiol Heart Circ Physiol* **2020**, *318* (3), H726.
(79) Grünberg, J.; Jeger, S.; Sarko, D.; Dennler, P.; Zimmermann, K.; Mier, W.; Schibli, R. DOTA-Functionalized Polylysine: A High Number of DOTA Chelates Positively Influences the Biodistribution of Enzymatic Conjugated Anti-Tumor Antibody ChCE7agl. *PLoS One* **2013**, *8* (4), No. e60350.
(80) Knogler, K.; Grünberg, J.; Novak-Hofer, I.; Zimmermann, K.; Schubiger, P. A. Evaluation of 177Lu-DOTA-Labeled Aglycosylated Monoclonal Anti-L1-CAM Antibody ChCE7: Influence of the Number of Chelators on the in Vitro and in Vivo Properties. *Nucl. Med. Biol.* **2006**, *33* (7), 883−889.
(81) Breeman, W. A. P.; van der Wansem, K.; Bernard, B. F.; van Gameren, A.; Erion, J. L.; Visser, T. J.; Krenning, E. P.; de Jong, M. The Addition of DTPA to [177Lu-DOTA0,Tyr3]Octreotate Prior to Administration Reduces Rat Skeleton Uptake of Radioactivity. *Eur. J. Nucl. Med. Mol. Imaging* **2003**, *30* (2), 312−315.
(82) Han, T. H.; Zhao, B. Absorption, Distribution, Metabolism, and Excretion Considerations for the Development of Antibody-Drug Conjugates. *Drug Metab. Dispos.* **2014**, *42* (11), 1914−1920.
(83) Alley, S. C.; Zhang, X.; Okeley, N. M.; Anderson, M.; Law, C.-L.; Senter, P. D.; Benjamin, D. R. The Pharmacologic Basis for Antibody-Auristatin Conjugate Activity. *J. Pharmacol. Exp. Ther.* **2009**, *330* (3), 932−938.

https://doi.org/10.1021/acs.jmedchem.1c02044
J. Med. Chem. 2022, 65, 6419−6430